Quinolone resistance genes *qnr*, *aac(6')-Ib-cr*, *oqxAB*, and *qepA* in environmental *Escherichia coli*: insights into their genetic contexts from comparative genomics

Ryota Gomi[a, *] and Fumie Adachi[b]

[a]Department of Environmental Engineering, Graduate School of Engineering, Kyoto University, Katsura, Nishikyo-ku, Kyoto 615-8540, Japan

[b]Department of Environmental Health, Osaka Institute of Public Health, 1-3-3 Nakamichi, Higashinari-ku, Osaka 537-0025, Japan

[*]Corresponding author

E-mail address: gomi.ryota.34v@kyoto-u.jp; Tel: +81-75-383-3354

Running title: Quinolone resistance genes in environmental *E. coli*

ABSTRACT

Previous studies have reported the occurrence of transferable quinolone resistance determinants in environmental *Escherichia coli*. However, little is known about their vectors and genetic contexts. To gain insights into these genetic characteristics, we analyzed the complete genomes of 53 environmental *E. coli* isolates, including 20 sequenced in this study and 33 sourced from RefSeq. The following transferable quinolone resistance determinants were detected: *qnrS1* (n = 33), *aac(6')-Ib-cr* (n = 12), *qnrS2* (n = 5), *oqxAB* (n = 4), *qnrB4* (n = 3), *qnrD1* (n = 3), *qnrB7* (n = 2), *qnrB19* (n = 2), *qepA1* (n = 1), and *qnrA1* (n = 1). These resistance genes were detected on plasmids of diverse replicon types; however, *aac(6')-Ib-cr*, *qnrS1*, and *qnrS2* were also detected on the chromosome. The genetic contexts surrounding these genes included not only those previously reported in clinical isolates but also novel contexts, such as *qnrD1* embedded within a composite transposon-like structure bounded by Tn*3*-derived inverted-repeat miniature elements (TIMEs). This study provides deep insights into mobile genetic elements associated with transferable quinolone resistance determinants, highlighting the importance of genomic surveillance of antimicrobial resistant bacteria in the environment.

Keywords: *Escherichia coli*, Antimicrobial resistance, Transferable mechanisms of quinolone resistance (TMQR), Plasmid-mediated quinolone resistance (PMQR), Genetic context

35 **INTRODUCTION**

36 *Escherichia coli* is a commensal member of the gut microbiota of humans and animals but can
37 also cause intestinal and extraintestinal infections.[1] Another concern besides pathogenicity is
38 the rise of antimicrobial resistance (AMR) in *E. coli*.[2] This is due to the accumulation of AMR
39 determinants, including acquired AMR genes and chromosomal point mutations.[3]

40 Quinolones are antibiotics that are widely used for treatment of infections caused by a variety
41 of bacteria, including *E. coli*.[4] Quinolone resistance in *E. coli* is mainly attributed to mutations
42 in the quinolone resistance-determining regions (QRDRs) of the topoisomerase genes *gyrA* and
43 *parC*.[5,6] Although these chromosomal mutations are generally not horizontally transferred,
44 there are quinolone resistance determinants that can be transmitted between bacteria, called
45 transferable mechanisms of quinolone resistance (TMQR).[7] These resistance determinants
46 include target protection (*qnr*), antibiotic efflux (mainly *qepA* and *oqxAB*), and antibiotic
47 modification (*aac(6')-Ib-cr* and *crpP*). Although these genes are usually called plasmid-
48 mediated quinolone resistance (PMQR) genes, the term PMQR is not always correct because
49 these transferable genes can sometimes be integrated into the chromosome (hence we use the
50 term TMQR, not PMQR, throughout this paper).[8] It is known that the levels of resistance
51 conferred by TMQR are relatively low; however, TMQR can play an important role in the
52 development of quinolone resistance because (i) the effect of TMQR on quinolone minimum
53 inhibitory concentrations (MICs) is additive to that conferred by other transferable or

54 chromosome-mediated quinolone resistance determinants, and (ii) TMQR can facilitate the
55 selection of mutants with higher-level quinolone resistance.[7,9]

56 Information on the vectors and genetic contexts of AMR genes is important for multiple
57 reasons: for example, (i) it allows identification of frequently associated/linked resistance
58 genes and thus can provide information on co-resistance; (ii) it facilitates better understanding
59 of their evolution and how resistance genes spread.[10,11] Although some previous studies
60 performed in-depth analysis of mobile elements carrying TMQR determinants in clinical *E.*
61 *coli*, limited information exists with respect to the vectors and genetic contexts of TMQR
62 determinants for environmental *E. coli*.[7,8] Here, we analyzed the complete genomes of
63 environmental *E. coli* isolates, sequenced in this study or obtained from the NCBI reference
64 sequence (RefSeq) database, with the aim to acquire genomic insights into TMQR, including
65 their vectors and genetic contexts.

66

67 **MATERIALS AND METHODS**

68 ***E. coli* isolates**

69 Twenty-four *E. coli* isolates obtained from surface water and wastewater in Japan were
70 characterized in this study. All these isolates were confirmed to carry TMQR determinants by
71 molecular methods such as PCR. These 24 isolates included 19 isolates from our previous

72 collections: (i) three isolates from river water samples collected in 2010,[12] (ii) 10 isolates from
73 river water samples collected between 2011–2013,[13] and (iii) six extended-spectrum β-
74 lactamase (ESBL)-producing *E. coli* isolates obtained from municipal wastewater and hospital
75 wastewater in 2015.[14] Five isolates were obtained in the present study: three isolates were
76 screened from *E. coli* isolated from municipal wastewater using CHROMagar ECC (Kanto
77 Chemical Co., Tokyo, Japan) supplemented with cefotaxime (1 mg/L) between 2019–2020,
78 and two isolates were screened from *E. coli* isolated from river water using CHROMagar ECC
79 supplemented with ciprofloxacin (0.03 mg/L) between 2021–2022. Antimicrobial
80 susceptibility testing of the 24 isolates was performed by microdilution using Dry Plate Eiken
81 (Eiken, Tokyo, Japan) according to CLSI specifications (see **Table S1** for antimicrobials used).
82 The MIC for ciprofloxacin was also determined using the Etest (bioMérieux, Marcy-l'Étoile,
83 France). The results were evaluated according to CLSI criteria[15] and EUCAST epidemiological
84 cutoff (ECOFF) values (https://mic.eucast.org/search/).

85 All 24 isolates were subjected to short- and long-read sequencing in the present study as
86 described below (note that short reads were obtained for some of the isolates in our previous
87 studies but we obtained short reads again in this work because the short reads in our previous
88 studies had low/uneven sequencing depth).

89 **Genome sequencing and assembly**

90 DNA was extracted from each isolate using a DNeasy PowerSoil Pro Kit (Qiagen, Hilden,
91 Germany). Short-read sequencing libraries were prepared using an Illumina DNA PCR-Free
92 Prep kit (Illumina, San Diego, CA). The libraries were sequenced on a NovaSeq 6000 platform
93 (Illumina), generating paired-end reads of 151 bp each. Long-read sequencing libraries were
94 prepared using the SQK-LSK109 kit (Oxford Nanopore Technologies, Oxford, UK) and
95 sequenced on the MinION with FLO-MIN106 flow cells.

96 Short reads were trimmed using fastp (v0.23.2),[16] and long reads were filtered using Filtlong
97 (v0.2.0, https://github.com/rrwick/Filtlong). Hybrid assembly was performed with a long-read-
98 first approach, i.e., long-read assembly using Flye (v2.9.1-b1780)[17] followed by long-read
99 polishing with Medaka (v1.8.0, https://github.com/nanoporetech/medaka) and short-read
100 polishing with Polypolish (v0.5.0).[18] Hybrid assembly was also performed with a short-read-
101 first approach using Unicycler (v0.5.0).[19] If the long-read-first approach generated a complete
102 genome, the polished Flye assembly was chosen as a final assembly. We note that long-read-
103 first assemblies sometimes lack small plasmids, so we recovered small plasmids that were not
104 present in the Flye assembly but were present in the Unicycler assembly.[20] If the long-read-
105 first approach did not generate a complete genome but the short-read-first approach did, the
106 Unicycler assembly was chosen as a final assembly.

107 If the above approaches failed to generate a complete genome, we performed long-read
108 sequencing again using DNA prepared from the same bacterial pellet but with a different

109 extraction method, which employs enzymatic digestion followed by proteinase K digestion and
110 AMPure XP (Beckman Coulter, Inc. Brea, CA, USA) bead purification, aiming to reduce DNA
111 shearing and to obtain longer reads. The obtained long reads with less fragmentation were
112 subjected to hybrid assembly as described above.

113 **Retrieving complete *E. coli* genomes with TMQR determinants from the NCBI database**

114 RefSeq *E. coli* genomes with an assembly level of "complete genome" (n = 2815) were
115 downloaded using the ncbi-genome-download tool (v0.3.1, https://github.com/kblin/ncbi-
116 genome-download) in July 2023. Metadata information, including strain name and isolation
117 source, was extracted from the downloaded files, and genomes determined to be of
118 environmental origin (i.e., surface water, sediment, wastewater, and soil) (n = 203) were
119 retained. AMR genes were detected using ABRicate (v1.0.1,
120 https://github.com/tseemann/abricate) with the NCBI database. This identified 48 genomes
121 with TMQR determinants. For each of the 48 genomes, we searched PubMed and Google
122 Scholar for the associated literature report. This identified literature reports for 33 genomes,
123 which were further analyzed in this study. Detailed information on these 33 genomes is
124 summarized in **Table S2**.

125 **Genomic analysis**

126 The *E. coli* genomes sequenced in this study and those retrieved from RefSeq were subjected
127 to the following genomic analysis. AMR genes were detected using ResFinder 4.1[21] and
128 ABRicate (v1.0.1, https://github.com/tseemann/abricate) with the NCBI database. Multilocus
129 sequence typing (MLST) was performed using mlst (v2.19.0,
130 https://github.com/tseemann/mlst). Plasmid replicons were detected using PlasmidFinder 2.1,
131 and plasmids were typed using pMLST 2.0.[22] Genomes were annotated using the RAST
132 server,[23] ISfinder,[24] and the BLAST algorithm (https://blast.ncbi.nlm.nih.gov/Blast.cgi). The
133 blastn analysis was performed using the nucleotide collection (nr/nt) database in April 2024.

134 **Data availability**

135 The complete genomes and sequence reads obtained in the present study have been deposited
136 in GenBank and the NCBI SRA under BioProject PRJNA1078256 (also see **Table 1** for the
137 nucleotide accession numbers of replicons with TMQR determinants). **Table S1** also
138 summarizes the nucleotide accession numbers of closed replicons for completed genomes and
139 SRA accession numbers for the remaining genomes.

140

141 **RESULTS AND DISCUSSION**

142 **Basic characteristics of *E. coli* isolates sequenced in this study**

143 Twenty-four *E. coli* isolates with TMQR determinants were sequenced in the present study.
144 These *E. coli* isolates were highly diverse and belonged to 20 different STs, including clinically
145 important lineages such as ST131 (**Table 1**). TMQR determinants detected include *qnrS1* (n =
146 12), *qnrD1* (n = 6), *aac(6')-Ib-cr* (n = 4), *qnrB7* (n = 3), *qnrS2* (n = 3), *qepA1* (n = 1), *qnrB19*
147 (n = 1), and *oqxAB* (n = 1) (**Table 1**). Five isolates carried multiple TMQR determinants: three
148 isolates carried *qnrB7* and *qnrD1*, one isolate carried *aac(6')-Ib-cr* and two copies of *qnrS2*,
149 and one isolate carried *aac(6')-Ib-cr*, *qnrS2*, and *oqxAB*.

150 Antimicrobial susceptibility testing revealed that the isolates were resistant to a wide variety
151 of antibiotics: nonsusceptibility rates ranged from 0% (piperacillin-tazobactam, ceftolozane-
152 tazobactam, cefmetazole, imipenem, meropenem, and amikacin) to 70.8% (ampicillin and
153 piperacillin) (**Table S1**). Nonsusceptibility rates for quinolones were 29.2% for nalidixic acid,
154 37.5% for ciprofloxacin (evaluated by Etest), and 37.5% for levofloxacin. All isolates were
155 non-susceptible to nalidixic acid, ciprofloxacin, and levofloxacin when they carried a QRDR
156 mutation(s). Isolates with TMQR determinants but without QRDR mutations were susceptible
157 to nalidixic acid but either susceptible or non-susceptible to ciprofloxacin and levofloxacin.
158 This is consistent with previous studies reporting that isolates with TMQR determinants but
159 without QRDR mutations sometimes show an unusual phenotype of nalidixic acid
160 susceptibility and ciprofloxacin resistance.[7] We also note that isolates with TMQR
161 determinants but without QRDR mutations were all classified as non-wild type to ciprofloxacin

162 and levofloxacin according to the ECOFF criteria, indicating that interpreting results with
163 ECOFF values can detect TMQR determinants when isolates do not carry QRDR mutations.

164 Of the 24 isolates, the genomes of 20 isolates could be completed, and these 20 completed
165 genomes were further analyzed to elucidate the genetic contexts of TMQR determinants.

166 **Basic characteristics of RefSeq *E. coli* genomes with TMQR determinants**

167 Thirty-three published RefSeq *E. coli* genomes with TMQR determinants were retrieved in the
168 present study. These were from wastewater (n = 18) or environmental water (n = 15), isolated
169 between 2012 and 2022, and from various geographical locations, with Switzerland (n = 14)
170 and Japan (n = 10) being dominant (**Table 2**). In total, 24 different STs were detected among
171 the genomes. The TMQR determinants detected include *qnrS1* (n = 21), *aac(6')-Ib-cr* (n = 9),
172 *qnrB4* (n = 3), *oqxAB* (n = 3), *qnrS2* (n = 2), *qnrA1* (n = 1), and *qnrB19* (n = 1). Six genomes
173 carried multiple TMQR determinants: three genomes carried *qnrS1* and *qnrS2*, one genome
174 carried *oqxAB* and *aac(6')-Ib-cr*, one genome carried *qnrB19* and *qnrS1*, and one genome
175 carried *aac(6')-Ib-cr*, *qnrB4*, and *qnrS1*.

176 **Genetic contexts of *qnr* genes**

177 A RefSeq genome analyzed in this study carried *qnrA1* on an IncA/C plasmid, p009_A. (*qnrA1*
178 was the first TMQR gene to be discovered, in 1998[25]). IS*CR1* is usually present upstream of
179 *qnrA1*, whereas downstream structures of *qnrA1* are known to be divergent.[26] In p009_A, the

180 structure IS*CR1-qnrA1-ampR-qacEΔ1-sul1-orf5-orf6*-IRt-IS*6100* was identified (**Figure 1**).

181 This structure was previously reported in the class 1 integrons In36 and In37,[27] though a

182 structure (*intI1-bla*$_{VIM-1}$*-aac(6')-II-dfrA1-ΔaadA-smr*-IS*Pa21*) seen in another class 1 integron,

183 In4873, was detected in the upstream region in p009_A.[28] The association of In4873, which

184 carries a *bla*$_{VIM}$ metallo-β-lactamase gene, and the *qnrA*-containing region in In36/In37 is

185 worrisome from a drug-resistance perspective but seems to be rare: blastn analysis found only

186 one closely related structure in plasmid pME-1a (CP041734.1) from a clinical *Enterobacter*

187 *hormaechei* isolate, which carried *bla*$_{VIM-4}$ instead of *bla*$_{VIM-1}$.

188 Three RefSeq genomes carried *qnrB4* on different IncF plasmids (F1:A1:B1, F2:A-:B-,

189 F31:F36:A4:B37). In one IncF plasmid (p142_A-OXA181 [F1:A1:B1]), a ColKP3 replicon

190 was also detected, but its *repA* gene was interrupted. *qnrB4* is known to be globally distributed

191 and often associated with the AmpC type β-lactamase gene *bla*$_{DHA-1}$.[26] In all three plasmids,

192 *bla*$_{DHA-1}$ was found upstream and a *ΔintI1-dfrA17-ΔaadA5* structure was identified downstream

193 of *qnrB4* (**Figure 2a**). In p53_A, the *ΔintI1-dfrA17-ΔaadA5* structure was inverted and the

194 *ΔintI1* sequence was 63-bp longer compared with the other two plasmids. Detection of the

195 (almost) identical genetic context in plasmids from Japan and Switzerland indicates a global

196 prevalence of this multiresistance region in environmental *E. coli*.

197 Two isolates sequenced to closure in the present study carried *qnrB7*. *qnrB7* was previously

198 reported to be associated with the ESBL gene *bla*$_{SHV-12}$.[26] However, reports of complete plasmid

199 (or chromosome) sequences carrying *qnrB7* are scarce; blastn analysis identified only four
200 complete plasmid sequences carrying *qnrB7*. One of them, the IncX3 plasmid
201 pLHST2018_IncX3 harbored by a clinical *Salmonella enterica* isolate from India, carried both
202 *qnrB7* and bla_{SHV-12}.[29] In our isolates, *qnrB7* was also carried by IncX3 plasmids and associated
203 with bla_{SHV-12} (**Figure 2b**). Various insertion sequences, including IS*26* and IS*3000*, and
204 remnants of transposons were found around *qnrB7* and bla_{SHV-12}, which seem to have
205 contributed to the mobilization of these resistance genes. Genetic contexts of *qnrB7* and bla_{SHV-}
206 $_{12}$ were almost identical in pKTa005_4 and pKFu015_3 except that a 1.9 kbp fragment of
207 IS*3000* was inserted next to another IS*3000* in pKTa005_4. The same genetic context was
208 identified in pLHST2018_IncX3 but was interrupted by IS*26* in *deoR*.

209 Two genomes, one sequenced by us and the other from RefSeq, carried *qnrB19*. *qnrB19* is
210 usually mobilized by transposition units (TPU) mediated by IS*Ecp1*, such as Tn*2012* and
211 Tn*5387*, or small ColE1-like plasmids containing fragments of these transposons.[30] The most
212 common *qnrB19*-carrying ColE1-like plasmid is a 2699 bp plasmid named pPAB19-
213 1/pSGI15/pECY6-7/pMK100, with others being minor variants of this plasmid.[30] The two
214 *qnrB19*-positive genomes carried this gene on small plasmids, p20A24_1 (3180 bp) and p32-
215 4_E (4417 bp), both with a ColE-like replicon Col(pHAD28).[31] These plasmids contained
216 putative ColE1-like *ori* (RNAI, RNAII, and *oriV*), *oriT*, and Xer sites (sites used for converting
217 plasmid multimers into monomers) (**Figure 2c**). p20A24_1 was found to be closely related to

218 plasmid pPAB19-3 (JN985534) from a clinical *E. coli* isolate, with some minor differences
219 (e.g., the Tn*5387* fragment was ~240bp longer in p20A24_1). p32-4_E was identified as a
220 cointegrate plasmid comprising the common *qnrB19*-carrying plasmid pPAB19-1 (GQ412195)
221 and a 1718 bp plasmid almost identical (single nucleotide difference) to pMB9272_7
222 (CP103528), with putative *oriT* regions being the cointegration points. pMB9272_7 carries
223 only two genes encoding hypothetical proteins, and no plasmid replicon was identified by
224 PlasmidFinder. Cointegrates comprising ColE1-like plasmids and large plasmids were
225 previously shown to play an important role in the evolution of AMR.[31] The example of p32-
226 4_E indicates cointegrates of ColE1-like plasmids and other small plasmids may also
227 contribute to the spread of AMR.

228 Three genomes sequenced to closure in the present study carried *qnrD1*. *qnrD1* was first
229 described on a 4270 bp plasmid, p2007057, in a clinical *Salmonella enterica* strain isolated in
230 China.[32] *qnrD1* has since been detected on multiple plasmids; however, blastn analysis
231 identified that *qnrD1* is rare in *Enterobacteriaceae* and mostly detected on ~2.7 kbp plasmids
232 in *Morganellaceae*. Two of the three genomes carried *qnrD1* on a plasmid identical to
233 p2007057 (**Figure 3**). This plasmid contains four ORFs, one of which is *mob*, in addition to
234 *qnrD1*. The remaining genome carried *qnrD1* on a 6657 bp plasmid, named pKFu015_4, with
235 no close blastn hits (all hits were below 50% query coverage). The *qnrD1* region, including
236 *qnrD1* and ORF2, in pKFu015_4 was identical to ~2.7 kbp *Morganellaceae* plasmids such as

237 pRS12-11 (KF364953) and was ~95% identical to the corresponding region in p2007057 (and
238 thus pKMi029_6 and pKTa005_7). This plasmid also carried regions corresponding to the *ori*,
239 *bom* (basis of mobility), *rom* (RNA one inhibition modulator), *mob*, and *cer* (ColE1 resolution
240 sequence) regions in plasmid ColE1.[33] Analysis of sequences surrounding the *qnrD1* region
241 revealed that there were 209 bp directly oriented repeats upstream and downstream of the
242 region. This repeat carried imperfect 33 bp inverted repeats (IRs) closely related to some Tn*3*-
243 family transposons (e.g., Tn*Ec4*), though it did not encode a transposase. The blastn analysis
244 revealed that this repeat is identical to a Tn*3*-derived inverted-repeat miniature element (TIME),
245 named $TIME_{IS\mathit{101}}$.[34] Pairs of TIMEs are known to be involved in mobilization of intervening
246 sequences when the corresponding Tn*3* family transposases are provided *in trans*, and these
247 composite transposon-like structures were previously named TIME-COMP.[34,35] Thus, the
248 TIME-COMP structure, $TIME_{IS\mathit{101}}$-*qnrD1*-ORF2-$TIME_{IS\mathit{101}}$, seems to have been mobilized as
249 a single unit into a ColE1-like plasmid, generating pKFu015_4. The presence of 5 bp direct
250 repeats (AGCTA) surrounding this structure supports this idea. Moreover, we also found a
251 ColE1-like plasmid without insertion of this TIME-COMP structure among the genomes
252 sequenced in this study (pKMi029_5, CP147114), further supporting this. *qnrD1* was
253 previously suggested to be mobilized as a mobile insertion cassette (mic) element (explained
254 below),[36] but this observation indicates another mode of *qnrD1* mobilization, namely TIME-
255 COMP.

256 *qnrS1* was the most prevalent TMQR gene both in our isolates (n = 12) and in RefSeq genomes
257 (n = 21), indicating the high prevalence of this gene in environmental *E. coli*. *qnrS1* was
258 detected on plasmids of diverse replicon types, and on the chromosome in two genomes (**Table**
259 **1** and **Table 2**). Analysis of the flanking sequences revealed that the genetic contexts of *qnrS1*
260 can largely be classified into 13 types (type A to type M in **Figure 4**). Types B, E, and I are the
261 contexts found only in the genomes analyzed in this study and no other hits were found by
262 blastn analysis. Type A is the context detected in the original *qnrS1*-harboring plasmid
263 pAH0376 from a clinical *Shigella flexneri* isolate and was also detected in five isolates
264 analyzed in this study (note that the available pAH0376 sequence ends at *tnpR* and the presence
265 of IS*Kpn19* in the plasmid is unknown).[37] Insertion of a TPU (IS*Ecp1*-$bla_{CTX-M-15}$-*Δorf477*) into
266 *tnpA* of Tn*2* in type A, which is a context prevalent in genomes deposited in GenBank (e.g.,
267 CP052151) but not detected in this study, seems to have been followed by (i) truncation of *tnpR*
268 by IS*26* (type B), (ii) transposition of a longer TPU, including the original TPU (IS*Ecp1*-bla_{CTX-}
269 $_{M-15}$-*Δorf477*) and the *qnrS1* region, into the chromosome by IS*Ecp1* (type C), or (iii) partial
270 deletion of Tn*2* and IS*Ecp1* and IS*26*-mediated truncation of IS*Kpn19* (type D). Truncation of
271 type A by two IS*26* elements might have led to generation of type E. IS*Kpn19* elements are
272 present both upstream and downstream of *qnrS1* in type F. The blastn analysis identified the
273 type F context in only two replicons, *E. coli* plasmid pA1.S1.126.c2 (CP146587) from human
274 urine and *E. coli* plasmid pKT58A (JX065631) from a wild bird in Slovakia.[38] In type G, IS*Ecl2*

275 is truncated by IS*26*, and class 1 integrons with different cassette arrays are present upstream
276 of *qnrS1*. The type H context contained the *ftsI-bla*$_{LAP-2}$-IS*Ecl2* structure upstream of *qnrS1*,
277 which was reported previously in clinical *Klebsiella pneumoniae* and was also detected in
278 multiple *Enterobacteriaceae* plasmids by blastn analysis.[39] Truncation of type H by IS*26* at
279 *bla*$_{LAP-2}$ seems to have given rise to type I. Type J and type K contexts are inserted in the same
280 position in each IncX1 plasmid and flanked by 5-bp direct repeats of ATAAC (or the reverse
281 complement sequence GTTAT). Insertion of Tn*2* in the ancestral IncX1 plasmid followed by
282 IS*26*-mediated rearrangements, including insertion of the region containing *qnrS1*, can explain
283 these contexts. Type L and Type M seem to have been derived from the *qnrS1*-bearing
284 transposon Tn*6292*. Tn*6292* itself was not detected in the present study, though blastn analysis
285 identified that intact Tn*6292* is almost restricted to *Enterobacteriaceae* plasmids from China.

286 Two genomes sequenced to closure in this study and two RefSeq genomes carried *qnrS2*. *qnrS2*
287 was previously reported to be part of a mic element bracketed by 22 bp imperfect IRs in the
288 *Aeromonas punctata* plasmid p37.[40] A mic element is a nonautonomous element bracketed by
289 two (imperfect) IRs. A mic does not carry a transposase gene but can be mobilized *in trans* by
290 a transposase that can recognize the IR. In two RefSeq genomes, *qnrS2* was embedded within
291 the same genetic context on IncX1 plasmids, but the mic element was truncated by IS*26*
292 (**Figure 5**). The IS*26*-*qnrS2*-*ΔmpR*-IS*26* structure, which was also detected in *E. coli* plasmids
293 such as pRW7-1_235k_tetX (MT219825), was followed by the *fosA3* genetic context type K,[41]

294 linking *qnrS2* to *fosA3*, *Δbla*$_{TEM}$, and *bla*$_{CTX-M-55}$. Two ST2179 genomes sequenced to closure

295 in this study carried *qnrS2* on the chromosome. In both genomes, *qnrS2* was within the

296 truncated mic element and was surrounded by directly-oriented IS*26* sequences. This IS*26*-

297 *qnrS2*-*ΔmpR*-IS*26* structure (note that this structure is different from that in the IncX1 plasmids,

298 in that the IS*26* sequences are directly-oriented and a ~200 bp fragment is present between the

299 truncated mic and the left IS*26*) was also detected in some *Enterobacteriaceae* plasmids such

300 as pSH16G4525 (MH522424). Interestingly, this *qnrS2* region was duplicated in 19M19. In

301 both ST2179 genomes, the *qnrS2* region was followed by *E. coli* chromosomal genes, but the

302 gene contents were different, likely due to the rearrangement caused by intramolecular

303 replicative transposition of IS*26*.[35]

304 **Genetic contexts of *aac(6')-Ib-cr***

305 Three genomes sequenced to closure in this study and nine RefSeq genomes carried *aac(6')-*

306 *Ib-cr*. Notably, *aac(6')-Ib-cr* was detected on the chromosome in six isolates (50%) belonging

307 to five different STs (ST10, ST410, ST648, ST1266, and ST2179). A chromosomal location

308 for *aac(6')-Ib-cr* was also reported previously in clinical ST131 and ST648 isolates from

309 Spain.[8] These examples indicate chromosomal integration of *aac(6')-Ib-cr* is frequent and has

310 occurred multiple times in different STs, again highlighting that the term PMQR is not

311 appropriate to describe transferable quinolone resistance genes. Plasmidic *aac(6')-Ib-cr* genes

312 were detected on different IncF plasmids (F1:A1:B16, F1:A1:B49, F10:A1:B49, F36:A4:B-,

313 F36:A4:B1, F47:A-:B75). One plasmid, pWP4-W18-ESBL-09_1 (F1:A1:B16), also carried a

314 Col156-like replicon, but the *repA* gene seems to be truncated.

315 *aac(6')-Ib-cr* has been identified in a gene cassette as part of class 1 integrons.[42] Although

316 *aac(6')-Ib-cr* is sometimes linked to the 5′-conserved segment (5′-CS) and the 3′-conserved

317 segment (3′-CS) in class 1 integrons, integrons containing *aac(6')-Ib-cr* are often interrupted

318 by IS*26*.[8,43] Our analysis supports this observation, having identified deletion/truncation of

319 either or both of 5′-CS and 3′-CS by IS*26* in 11 of 12 cases (**Figure 6**). Apparently, the

320 truncated structures seen in the 11 genomes were derived from the class 1 integron *intI1-*

321 *aac(6')-Ib-cr-bla*$_{OXA-1}$*-catB3-arr-3-qacEΔ1-sul1*. Among them, the IS*26-aac(6')-Ib-cr-bla*$_{OXA-}$

322 $_{1}$*-ΔcatB3*-IS*26* structure was prevalent and detected in seven genomes (58%), while the

323 upstream and downstream sequences were divergent. The blastn analysis revealed that this

324 structure is prevalent among the public genomes (more than 1000 hits with >99% coverage and

325 with >99% identity). It should be noted, however, that the IS*26* sequences are inversely

326 oriented and thus this structure is neither a transposon nor a pseudo compound transposon.[44]

327 The prevalence of this structure among various plasmids/chromosomes can partially be

328 explained by the presence of other mobile genetic elements surrounding it, which might have

329 aided the movement of multiresistance regions containing this structure.

330 **Genetic contexts of *oqxAB***

331 Mobile *oqxAB* genes are commonly found within the IS*26*-*oqxA*-*oqxB*-*oqxR*-IS*26* structure,

332 named Tn*6010*.[45] All four *oqxAB* genes identified in the present study were situated within

333 Tn*6010* (or a truncated Tn*6010*) and carried by plasmids of different Inc types (**Figure 7**).

334 While the downstream sequences flanking Tn*6010* were divergent in the four plasmids, three

335 RefSeq plasmids carried common sequences upstream of Tn*6010*, containing *tnpA* of Tn*2*,

336 IS*26*, *bleO*, *nimC*/*nimA,* and *Δ*IS*Enca1*. The blastn analysis using this upstream structure +

337 Tn*6010* as a query sequence identified more than 100 genomes carrying this structure. On the

338 other hand, the upstream structure of Tn*6010* was replaced by a truncated Tn*1721* and a

339 truncated Tn*2* in pJKHS004_1, linking *tetA* and a truncated bla_{TEM} to *oqxAB*. No genomes were

340 found by blastn analysis to carry the multiresistance region detected in pJKHS004_1.

341 **Genetic context of *qepA1***

342 *qepA* genes are typically associated with IS*CR3* and embedded within complex integrons.[46]

343 One isolate sequenced in this study carried *qepA1*, and the gene was located between a

344 truncated *intI1* and IS*CR3* on an incF plasmid (C4:F18:A-:B1), pKMi012_1 (**Figure 8**). This

345 region was followed by a *ΔintI1*/*groEL-dfrB4-qacEΔ1-sul1-Δorf5* region, the chromate

346 resistance (*chrA*) region, and the macrolide resistance (*mph*(A)) region. The blastn analysis of

347 the entire resistance region bounded by IS*26* revealed almost identical sequences (100% query

348 coverage and >99% identity) in three *E. coli* plasmids, namely pJJ1887-5 (CP014320.1) from

349 a clinical isolate in the USA, pM216_mF (LC492469.1) from a clinical isolate in Myanmar,

350 and pMyNCGM604 (LC744503.1) from an isolate of unknown origin in Myanmar, indicating
351 a wide distribution of this multiresistance region.

352 **Study limitations**

353 This study has some limitations. The genomes of four isolates (KMi014, KTa007, KTa009,
354 JKHS019) could not be completed despite repeated long-read sequencing. This is probably due
355 to the presence of long repeats in these genomes. We also included RefSeq genomes in our
356 analysis to extend our dataset, but most RefSeq genomes were from Japan and Switzerland.
357 This seems to reflect the situation where long-read sequencing is still not widely used to study
358 antibiotic resistance in environmental bacteria.

359

360 **CONCLUSIONS**

361 Here, we performed in-depth analysis of the genetic contexts of TMQR determinants in
362 environmental *E. coli*. The genetic contexts described in this study included those closely
363 related to the contexts previously reported in clinical isolates. We also detected novel genetic
364 contexts, such as *qnrD1* embedded within TIME-COMP. Some of the TMQR genes were
365 frequently associated with other AMR genes in the described contexts (e.g., *qnrB7* and bla_{SHV-}
366 $_{12}$), and this information will contribute to our understanding of how multidrug resistance
367 emerges in bacteria. We also found that certain TMQR determinants (i.e., *qnrS1*, *qnrS2*, and

368 *aac(6')-Ib-cr*) are located not only on plasmids but also on the chromosome, encouraging the
369 use of the term TMQR rather than PMQR to avoid erroneous interpretations in future studies.
370 Overall, this study provides valuable insights into mobile genetic elements associated with
371 TMQR determinants and highlights the importance of genomic surveillance of antimicrobial
372 resistant bacteria in the environment.

373

374 **ACKNOWLEDGEMENTS**

375 This work was supported by JSPS KAKENHI (grant number JP22K18038), the Kurita Water
376 and Environment Foundation (22B006), the Sumitomo Foundation (2230113), and the
377 Environment Research and Technology Development Fund (JPMEERF20235R01) of the
378 Environmental Restoration and Conservation Agency, provided by the Ministry of the
379 Environment of Japan. Computations were partially performed on the NIG supercomputer at
380 ROIS National Institute of Genetics. We acknowledge the NGS core facility of the Genome
381 Information Research Center at the Research Institute for Microbial Diseases of Osaka
382 University for the support in DNA sequencing. We also thank Isao Nakamoto and Yasufumi
383 Matsumura for their support in antimicrobial susceptibility testing.

384 **AUTHOR CONTRIBUTIONS**

385 Conceptualization: R.G.; methodology: R.G.; validation: R.G.; formal analysis: R.G.;
386 investigation: R.G. and F.A; resources: R.G. and F.A; data curation: R.G.; visualization: R.G.;
387 writing – original draft: R.G.; writing – review & editing: R.G. and F.A.

388

389 References

390 1 Kaper, J. B., Nataro, J. P. & Mobley, H. L. Pathogenic *Escherichia coli*. *Nat Rev*
391 *Microbiol* **2**, 123-140 (2004). https://doi.org/10.1038/nrmicro818
392 2 Denamur, E., Clermont, O., Bonacorsi, S. & Gordon, D. The population genetics of
393 pathogenic *Escherichia coli*. *Nat Rev Microbiol* **19**, 37-54 (2021).
394 https://doi.org/10.1038/s41579-020-0416-x
395 3 Poirel, L. *et al*. Antimicrobial Resistance in *Escherichia coli*. *Microbiol Spectr* **6** (2018).
396 https://doi.org/10.1128/microbiolspec.ARBA-0026-2017
397 4 Aldred, K. J., Kerns, R. J. & Osheroff, N. Mechanism of quinolone action and resistance.
398 *Biochemistry* **53**, 1565-1574 (2014). https://doi.org/10.1021/bi5000564
399 5 Aoike, N. *et al*. Molecular characterization of extraintestinal *Escherichia coli* isolates
400 in Japan: relationship between sequence types and mutation patterns of quinolone
401 resistance-determining regions analyzed by pyrosequencing. *J Clin Microbiol* **51**,
402 1692-1698 (2013). https://doi.org/10.1128/JCM.03049-12
403 6 van der Putten, B. C. L. *et al*. Quantifying the contribution of four resistance
404 mechanisms to ciprofloxacin MIC in *Escherichia coli*: a systematic review. *J*
405 *Antimicrob Chemother* **74**, 298-310 (2019). https://doi.org/10.1093/jac/dky417
406 7 Ruiz, J. Transferable Mechanisms of Quinolone Resistance from 1998 Onward. *Clin*
407 *Microbiol Rev* **32** (2019). https://doi.org/10.1128/CMR.00007-19
408 8 Ruiz, E. *et al*. *qnr*, *aac(6')-Ib-cr* and *qepA* genes in *Escherichia coli* and *Klebsiella* spp.:
409 genetic environments and plasmid and chromosomal location. *J Antimicrob Chemother*
410 **67**, 886-897 (2012). https://doi.org/10.1093/jac/dkr548
411 9 Hooper, D. C. & Jacoby, G. A. Mechanisms of drug resistance: quinolone resistance.
412 *Ann N Y Acad Sci* **1354**, 12-31 (2015). https://doi.org/10.1111/nyas.12830
413 10 Partridge, S. R. Analysis of antibiotic resistance regions in Gram-negative bacteria.
414 *FEMS Microbiol Rev* **35**, 820-855 (2011). https://doi.org/10.1111/j.1574-
415 6976.2011.00277.x
416 11 Partridge, S. R. & Tsafnat, G. Automated annotation of mobile antibiotic resistance in
417 Gram-negative bacteria: the Multiple Antibiotic Resistance Annotator (MARA) and

418 database. *J Antimicrob Chemother* **73**, 883-890 (2018).
419 https://doi.org/10.1093/jac/dkx513
420 12 Adachi, F., Yamamoto, A., Takakura, K. & Kawahara, R. Occurrence of
421 fluoroquinolones and fluoroquinolone-resistance genes in the aquatic environment. *Sci*
422 *Total Environ* **444**, 508-514 (2013). https://doi.org/10.1016/j.scitotenv.2012.11.077
423 13 Gomi, R. *et al*. Whole-Genome Analysis of Antimicrobial-Resistant and Extraintestinal
424 Pathogenic *Escherichia coli* in River Water. *Appl Environ Microbiol* **83** (2017).
425 https://doi.org/10.1128/AEM.02703-16
426 14 Gomi, R. *et al*. Occurrence of Clinically Important Lineages, Including the Sequence
427 Type 131 C1-M27 Subclone, among Extended-Spectrum-beta-Lactamase-Producing
428 *Escherichia coli* in Wastewater. *Antimicrob Agents Chemother* **61** (2017).
429 https://doi.org/10.1128/AAC.00564-17
430 15 CLSI. Performance Standards for Antimicrobial Susceptibility Testing—Thirtieth
431 Edition: M100. (2020).
432 16 Chen, S., Zhou, Y., Chen, Y. & Gu, J. fastp: an ultra-fast all-in-one FASTQ
433 preprocessor. *Bioinformatics* **34**, i884-i890 (2018).
434 https://doi.org/10.1093/bioinformatics/bty560
435 17 Kolmogorov, M., Yuan, J., Lin, Y. & Pevzner, P. A. Assembly of long, error-prone
436 reads using repeat graphs. *Nat Biotechnol* **37**, 540-546 (2019).
437 https://doi.org/10.1038/s41587-019-0072-8
438 18 Wick, R. R. & Holt, K. E. Polypolish: Short-read polishing of long-read bacterial
439 genome assemblies. *PLoS Comput Biol* **18**, e1009802 (2022).
440 https://doi.org/10.1371/journal.pcbi.1009802
441 19 Wick, R. R., Judd, L. M., Gorrie, C. L. & Holt, K. E. Unicycler: Resolving bacterial
442 genome assemblies from short and long sequencing reads. *PLoS Comput Biol* **13**,
443 e1005595 (2017). https://doi.org/10.1371/journal.pcbi.1005595
444 20 Wick, R. R., Judd, L. M. & Holt, K. E. Assembling the perfect bacterial genome using
445 Oxford Nanopore and Illumina sequencing. *PLoS Comput Biol* **19**, e1010905 (2023).
446 https://doi.org/10.1371/journal.pcbi.1010905
447 21 Bortolaia, V. *et al*. ResFinder 4.0 for predictions of phenotypes from genotypes. *J*
448 *Antimicrob Chemother* **75**, 3491-3500 (2020). https://doi.org/10.1093/jac/dkaa345
449 22 Carattoli, A. *et al*. *In silico* detection and typing of plasmids using PlasmidFinder and
450 plasmid multilocus sequence typing. *Antimicrob Agents Chemother* **58**, 3895-3903
451 (2014). https://doi.org/10.1128/AAC.02412-14
452 23 Aziz, R. K. *et al*. The RAST Server: rapid annotations using subsystems technology.
453 *BMC Genomics* **9**, 75 (2008). https://doi.org/10.1186/1471-2164-9-75

454 24 Siguier, P., Perochon, J., Lestrade, L., Mahillon, J. & Chandler, M. ISfinder: the
455 reference centre for bacterial insertion sequences. *Nucleic Acids Res* **34**, D32-36 (2006).
456 https://doi.org/10.1093/nar/gkj014
457 25 Martinez-Martinez, L., Pascual, A. & Jacoby, G. A. Quinolone resistance from a
458 transferable plasmid. *Lancet* **351**, 797-799 (1998). https://doi.org/10.1016/S0140-
459 6736(97)07322-4
460 26 Strahilevitz, J., Jacoby, G. A., Hooper, D. C. & Robicsek, A. Plasmid-mediated
461 quinolone resistance: a multifaceted threat. *Clin Microbiol Rev* **22**, 664-689 (2009).
462 https://doi.org/10.1128/CMR.00016-09
463 27 Wang, M. *et al*. Plasmid-mediated quinolone resistance in clinical isolates of
464 *Escherichia coli* from Shanghai, China. *Antimicrob Agents Chemother* **47**, 2242-2248
465 (2003). https://doi.org/10.1128/AAC.47.7.2242-2248.2003
466 28 Papagiannitsis, C. C. *et al*. Survey of metallo-beta-lactamase-producing
467 Enterobacteriaceae colonizing patients in European ICUs and rehabilitation units,
468 2008-11. *J Antimicrob Chemother* **70**, 1981-1988 (2015).
469 https://doi.org/10.1093/jac/dkv055
470 29 Jacob, J. J. *et al*. *Salmonella* Typhi acquires diverse plasmids from other
471 Enterobacteriaceae to develop cephalosporin resistance. *Genomics* **113**, 2171-2176
472 (2021). https://doi.org/10.1016/j.ygeno.2021.05.003
473 30 Tran, T. *et al*. Small plasmids harboring *qnrB19*: a model for plasmid evolution
474 mediated by site-specific recombination at *oriT* and Xer sites. *Antimicrob Agents*
475 *Chemother* **56**, 1821-1827 (2012). https://doi.org/10.1128/AAC.06036-11
476 31 Ares-Arroyo, M., Rocha, E. P. C. & Gonzalez-Zorn, B. Evolution of ColE1-like
477 plasmids across gamma-Proteobacteria: From bacteriocin production to antimicrobial
478 resistance. *PLoS Genet* **17**, e1009919 (2021).
479 https://doi.org/10.1371/journal.pgen.1009919
480 32 Cavaco, L. M., Hasman, H., Xia, S. & Aarestrup, F. M. *qnrD*, a novel gene conferring
481 transferable quinolone resistance in *Salmonella enterica* serovar Kentucky and
482 Bovismorbificans strains of human origin. *Antimicrob Agents Chemother* **53**, 603-608
483 (2009). https://doi.org/10.1128/AAC.00997-08
484 33 Chan, P. T., Ohmori, H., Tomizawa, J. & Lebowitz, J. Nucleotide sequence and gene
485 organization of ColE1 DNA. *J Biol Chem* **260**, 8925-8935 (1985).
486 34 Szuplewska, M., Ludwiczak, M., Lyzwa, K., Czarnecki, J. & Bartosik, D. Mobility and
487 generation of mosaic non-autonomous transposons by Tn*3*-derived inverted-repeat
488 miniature elements (TIMEs). *PLoS One* **9**, e105010 (2014).
489 https://doi.org/10.1371/journal.pone.0105010

35 Partridge, S. R., Kwong, S. M., Firth, N. & Jensen, S. O. Mobile Genetic Elements Associated with Antimicrobial Resistance. *Clin Microbiol Rev* **31** (2018). https://doi.org/10.1128/CMR.00088-17

36 Guillard, T. *et al*. Mobile insertion cassette elements found in small non-transmissible plasmids in *Proteeae* may explain *qnrD* mobilization. *PLoS One* **9**, e87801 (2014). https://doi.org/10.1371/journal.pone.0087801

37 Hata, M. *et al*. Cloning of a novel gene for quinolone resistance from a transferable plasmid in *Shigella flexneri* 2b. *Antimicrob Agents Chemother* **49**, 801-803 (2005). https://doi.org/10.1128/AAC.49.2.801-803.2005

38 Dolejska, M., Villa, L., Hasman, H., Hansen, L. & Carattoli, A. Characterization of IncN plasmids carrying $bla_{\text{CTX-M-1}}$ and *qnr* genes in *Escherichia coli* and *Salmonella* from animals, the environment and humans. *J Antimicrob Chemother* **68**, 333-339 (2013). https://doi.org/10.1093/jac/dks387

39 Karah, N. *et al*. Plasmid-mediated quinolone resistance determinants *qnr* and *aac(6')-Ib-cr* in *Escherichia coli* and *Klebsiella* spp. from Norway and Sweden. *Diagn Microbiol Infect Dis* **66**, 425-431 (2010). https://doi.org/10.1016/j.diagmicrobio.2009.12.004

40 Cattoir, V., Poirel, L., Aubert, C., Soussy, C. J. & Nordmann, P. Unexpected occurrence of plasmid-mediated quinolone resistance determinants in environmental *Aeromonas* spp. *Emerg Infect Dis* **14**, 231-237 (2008). https://doi.org/10.3201/eid1402.070677

41 Lv, L. *et al*. Multiple Plasmid Vectors Mediate the Spread of *fosA3* in Extended-Spectrum-beta-Lactamase-Producing *Enterobacterales* Isolates from Retail Vegetables in China. *mSphere* **5** (2020). https://doi.org/10.1128/mSphere.00507-20

42 Rodriguez-Martinez, J. M. *et al*. Plasmid-mediated quinolone resistance: Two decades on. *Drug Resist Updat* **29**, 13-29 (2016). https://doi.org/10.1016/j.drup.2016.09.001

43 Partridge, S. R., Zong, Z. & Iredell, J. R. Recombination in IS*26* and Tn*2* in the evolution of multiresistance regions carrying $bla_{\text{CTX-M-15}}$ on conjugative IncF plasmids from *Escherichia coli*. *Antimicrob Agents Chemother* **55**, 4971-4978 (2011). https://doi.org/10.1128/AAC.00025-11

44 Harmer, C. J., Pong, C. H. & Hall, R. M. Structures bounded by directly-oriented members of the IS*26* family are pseudo-compound transposons. *Plasmid* **111**, 102530 (2020). https://doi.org/10.1016/j.plasmid.2020.102530

45 Norman, A., Hansen, L. H., She, Q. & Sorensen, S. J. Nucleotide sequence of pOLA52: a conjugative IncX1 plasmid from *Escherichia coli* which enables biofilm formation and multidrug efflux. *Plasmid* **60**, 59-74 (2008). https://doi.org/10.1016/j.plasmid.2008.03.003

46 Cattoir, V., Poirel, L. & Nordmann, P. Plasmid-mediated quinolone resistance pump QepA2 in an *Escherichia coli* isolate from France. *Antimicrob Agents Chemother* **52**, 3801-3804 (2008). https://doi.org/10.1128/AAC.00638-08

47 Lin, Y. *et al*. Metadata Analysis of mcr-1-Bearing Plasmids Inspired by the Sequencing Evidence for Horizontal Transfer of Antibiotic Resistance Genes Between Polluted River and Wild Birds. *Front Microbiol* **11**, 352 (2020). https://doi.org/10.3389/fmicb.2020.00352

48 Long, H. *et al*. The co-transfer of plasmid-borne colistin-resistant genes *mcr-1* and *mcr-3.5*, the carbapenemase gene $bla_{\text{NDM-5}}$ and the 16S methylase gene *rmtB* from *Escherichia coli*. *Sci Rep* **9**, 696 (2019). https://doi.org/10.1038/s41598-018-37125-1

49 Che, Y. *et al*. High-resolution genomic surveillance elucidates a multilayered hierarchical transfer of resistance between WWTP- and human/animal-associated bacteria. *Microbiome* **10**, 16 (2022). https://doi.org/10.1186/s40168-021-01192-w

50 Ju, X., Wu, Y., Chen, G. & Zhang, R. *Escherichia coli* high-risk clone ST410 harboring $bla_{\text{NDM-13}}$ isolated from hospital wastewater in China. *Environ Sci Pollut Res Int* **30**, 91487-91491 (2023). https://doi.org/10.1007/s11356-023-28193-6

51 Gomi, R., Yamamoto, M., Tanaka, M. & Matsumura, Y. Chromosomal integration of $bla_{\text{CTX-M}}$ genes in diverse *Escherichia coli* isolates recovered from river water in Japan. *Curr Res Microb Sci* **3**, 100144 (2022). https://doi.org/10.1016/j.crmicr.2022.100144

52 Sekizuka, T., Inamine, Y., Segawa, T. & Kuroda, M. Characterization of NDM-5- and CTX-M-55-coproducing *Escherichia coli* GSH8M-2 isolated from the effluent of a wastewater treatment plant in Tokyo Bay. *Infect Drug Resist* **12**, 2243-2249 (2019). https://doi.org/10.2147/IDR.S215273

53 Sekizuka, T., Tanaka, R., Hashino, M., Yatsu, K. & Kuroda, M. Comprehensive Genome and Plasmidome Analysis of Antimicrobial Resistant Bacteria in Wastewater Treatment Plant Effluent of Tokyo. *Antibiotics (Basel)* **11** (2022). https://doi.org/10.3390/antibiotics11101283

54 Finton, M. D., Meisal, R., Porcellato, D., Brandal, L. T. & Lindstedt, B. A. Whole Genome Sequencing and Characterization of Multidrug-Resistant (MDR) Bacterial Strains Isolated From a Norwegian University Campus Pond. *Front Microbiol* **11**, 1273 (2020). https://doi.org/10.3389/fmicb.2020.01273

55 Biggel, M., Zurfluh, K., Treier, A., Nuesch-Inderbinen, M. & Stephan, R. Characteristics of *fosA*-carrying plasmids in *E. coli* and *Klebsiella* spp. isolates originating from food and environmental samples. *J Antimicrob Chemother* **76**, 2004-2011 (2021). https://doi.org/10.1093/jac/dkab119

56 Bleichenbacher, S. *et al*. Environmental dissemination of carbapenemase-producing Enterobacteriaceae in rivers in Switzerland. *Environ Pollut* **265**, 115081 (2020). https://doi.org/10.1016/j.envpol.2020.115081

564 57 Kurekci, C. *et al*. Emergence and Characterization of Tigecycline Resistance Gene
565 *tet*(X4) in ST609 *Escherichia coli* Isolates from Wastewater in Turkey. *Microbiol*
566 *Spectr* **10**, e0073222 (2022). https://doi.org/10.1128/spectrum.00732-22
567 58 Liedhegner, E. *et al*. Similarities in Virulence and Extended Spectrum Beta-Lactamase
568 Gene Profiles among Cefotaxime-Resistant *Escherichia coli* Wastewater and Clinical
569 Isolates. *Antibiotics (Basel)* **11** (2022). https://doi.org/10.3390/antibiotics11020260

570

571

572

573 **TABLES**

574 **Table 1.** Characteristics of 24 *E. coli* isolates sequenced in this study[a]

Isolate	Source	Year of isolation	ST	TMQR determinant(s)[b]	Replicon with TMQR determinant(s) (size, nucleotide accession number)	QRDRs[c]
1002W03	river water	2010	ST91	*qnrS1* (type F)	IncN plasmid (43766 bp, CP147054)	SDSE (0)
1008S13	river water	2010	ST1141	*qnrS1* (type I)	IncF plasmid (65333 bp, CP147052)	SDSE (0)
1008S19	river water	2010	ST216	*qnrS1* (type H)	IncF/IncN plasmid (50257 bp, CP147051)	SDSE (0)
KFu015	river water	2011	ST215	*qnrB7, qnrD1*	*qnrB7*: IncX3 plasmid (46557 bp, CP147133) *qnrD1*: Col3M/ColRNAI plasmid (6657 bp, CP147134)	SDSE (0)
KMi012	river water	2011	ST46	*qepA1*	IncF plasmid (140174 bp, CP147126)	LNIE (3)
KMi029	river water	2011	ST216	*qnrD1*	Col3M plasmid (4270 bp, CP147115)	SDSE (0)
KMi014[d]	river water	2011	ST607	*qnrB7, qnrD1*	-	SDSE (0)
KKa014	river water	2012	ST58	*qnrS1* (type A)	IncY plasmid (131602 bp, CP147106)	SDSE (0)
KFu021	river water	2012	ST58	*qnrS1* (type A)	IncY plasmid (130264 bp, CP147102)	SDSE (0)
KOr024	river water	2013	ST101	*qnrS1* (type J)	IncX1 plasmid (41491 bp, CP147097)	SDSE (0)

KTa005	river water	2013	ST542	*qnrB7, qnrD1*	*qnrB7*: IncX3 plasmid (48469 bp, CP147088) *qnrD1*: Col3M plasmid (4270 bp, CP147091)	SDSE (0)
KTa007[d]	river water	2013	ST218	*qnrD1*	-	SDSE (0)
KTa009[d]	river water	2013	ST218	*qnrD1*	-	SDSE (0)
JSWP006	municipal wastewater	2015	ST393	*qnrS1* (type E)	IncF plasmid (123573 bp, CP147082)	LNIE (3)
JSWP021	municipal wastewater	2015	ST224	*aac(6')-Ib-cr*	IncF plasmid (120365 bp, CP147076)	LNIE (3)
JKHS004	hospital wastewater	2015	ST2179	*qnrS2, aac(6')-Ib-cr, oqxA, oqxB*	*qnrS2, aac(6')-Ib-cr*: chromosome (4949596 bp, CP147069) *oqxA, oqxB*: IncF plasmid (143870 bp, CP147070)	LDIE (2)
JKHS006	hospital wastewater	2015	ST131	*qnrS1* (type L)	IncN plasmid (63327 bp, CP147064)	LDSE (1)
JKHS016	hospital wastewater	2015	ST43	*qnrS1* (type D)	IncI1-I(Alpha) plasmid (100666 bp, CP147060)	SDSE (0)
JKHS019[d]	hospital wastewater	2015	ST410	*aac(6')-Ib-cr*	-	LNIE (3)
19M19	municipal wastewater	2019	ST2179	*qnrS2* (two copies), *aac(6')-Ib-cr*	*qnrS2* (two copies), *aac(6')-Ib-cr*: chromosome (4870130 bp, CP147048)	LDIE (2)
19A14	municipal wastewater	2019	ST38	*qnrS1* (type C)	chromosome (4879959 bp, CP147046)	SDSE (0)
20A24	municipal wastewater	2020	ST10	*qnrB19*	Col(pHAD28) plasmid (3180 bp, CP147045)	SDSE (0)

21F61	river water	2021	ST657	*qnrS1* (type J)	IncX1 plasmid (48446 bp, CP147040)	SDSE (0)
22F46	river water	2022	ST540	*qnrS1* (type A)	IncF plasmid (100207 bp, CP147033)	SDSE (0)

575 [a]Detailed information on each isolate, such as other AMR genes detected, is available in **Table**

576 **S1**.

577 [b]The context type is shown for *qnrS1*.

578 [c]GyrA codons 83 and 87 and ParC codons 80 and 84 are shown in this order. SDSE is the wild-

579 type. The number of amino acid substitutions is shown in parentheses.

580 [d]The genomes of these four isolates could not be completed.

581

582

583 **Table 2.** Characteristics of 33 RefSeq *E. coli* genomes with TMQR determinants[a]

Isolate[(reference)]	Source	Location	Year of isolation	ST	TMQR determinant(s)[b]	Replicon with TMQR determinant(s) (size, nucleotide accession number)	QRDRs[c]
W5-6[47]	river water	China	2015	ST744	*oqxA, oqxB*	IncHI2/IncHI2A plasmid (241043 bp, NZ_CP032993.1)	LNIE (3)
WCHEC025943[48]	hospital wastewater	China	2017	ST410	*oqxA, oqxB, aac(6')-Ib-cr*	*oqxA*, *oqxB*: IncHI2/IncHI2A/IncN plasmid (265538 bp, NZ_CP027202.2) *aac(6')-Ib-cr*: IncF plasmid (75779 bp, NZ_CP027200.1)	LNIE (3)
SWHEFF_58[49]	municipal wastewater	China	2018	ST38	*qnrS1* (type K)	IncX1 plasmid (46569 bp, NZ_CP055050.1)	SDSE (0)
STLEFF_47[49]	municipal wastewater	China	2018	ST117	*qnrS1* (type G)	IncI1-I(Alpha) plasmid, (121650 bp, NZ_CP058876.1)	SDSE (0)
C-SRM-3[50]	hospital wastewater	China	2022	ST410	*aac(6')-Ib-cr*	chromosome (4799348 bp, NZ_CP123197.1)	LNIE (3)
KFu023[51]	river water	Japan	2013	ST10	*aac(6')-Ib-cr*	chromosome (4672002 bp, NZ_CP091662.1)	LNIE (3)

GSH8M-2[52]	municipal wastewater	Japan	2018	ST542	*qnrS1* (type G), *qnrS2*	*qnrS1*: IncF plasmid (145389 bp, NZ_AP019676.1) *qnrS2*: IncX1 plasmid (49365 bp, NZ_AP019678.1)	SDSE (0)
WP5-S17-ESBL-11[53]	municipal wastewater	Japan	2017	ST58	*qnrS1* (type C)	chromosome (4781831 bp, NZ_AP022107.1)	SDSE (0)
WP2-W18-CRE-03[53]	municipal wastewater	Japan	2018	ST602	*oqxA, oqxB*	IncF/IncQ1 plasmid (158754 bp, NZ_AP021915.1)	LNIE (3)
WP4-W18-ESBL-09[53]	municipal wastewater	Japan	2018	ST405	*aac(6')-Ib-cr*	IncF/Col156 plasmid (117617 bp, NZ_AP022070.1)	LNIE (3)
WP7-S17-ESBL-04[53]	municipal wastewater	Japan	2017	ST10	*qnrS1* (type B)	IncF/IncN plasmid (123262 bp, NZ_AP022178.1)	SDSE (0)
WP8-S17-ESBL-05[53]	municipal wastewater	Japan	2017	ST641	*qnrS1* (type G)	IncX1 plasmid (53216 bp, NZ_AP022218.1)	SDSE (0)
WP8-S18-CRE-02[53]	municipal wastewater	Japan	2018	ST542	*qnrS1* (type G), *qnrS2*	*qnrS1*: IncF plasmid (145389 bp, NZ_AP022246.1)	SDSE (0)

						qnrS2: IncX1 plasmid (49365 bp, NZ_AP022248.1)	
WP8-S18-ESBL-07[53]	municipal wastewater	Japan	2018	ST2858	*qnrS1* (type D)	IncB/O/K/Z plasmid (91233 bp, NZ_AP022263.1)	SDSE (0)
BEC1-S17-ESBL-09[53]	sea water	Japan	2017	ST130	*qnrB4*	IncF plasmid (83140 bp, NZ_AP022300.1)	LDSE (1)
NMBU_W12E19[54]	surface water	Norway	2019	ST1286	*qnrS1* (type D)	IncI1-I(Alpha) plasmid (88772 bp, NZ_CP042886.1)	SDSE (0)
OW1E2[55]	surface water	Switzerland	2012	ST11280	*qnrS1* (type H)	IncF plasmid (74070 bp, NZ_CP067247.1)	LDSE (1)
ABW_S38[55]	wastewater	Switzerland	2015	ST215	*qnrS1* (type H)	IncF plasmid (53010 bp, NZ_CP067268.1)	SDSE (0)
027_SK3[55]	wastewater	Switzerland	2016	ST215	*qnrS1* (type H)	IncF plasmid (104584 bp, NZ_CP067313.1)	SDSE (0)
ABW_A19[55]	wastewater	Switzerland	2015	ST1266	*aac(6')-Ib-cr*	chromosome (5250599 bp, NZ_CP067307.1)	LNIE (3)
CF009[56]	surface water	Switzerland	2019	ST73	*qnrA1*	IncA/C plasmid (159959 bp, NZ_CP048305.1)	SDSE (0)
CF032[56]	surface water	Switzerland	2019	ST1284	*qnrB19, qnrS1* (type M)	*qnrB19*: Col(pHAD28) plasmid (4417 bp, NZ_CP048315.1)	LNIE (3)

						qnrS1: IncX3/ColKP3 plasmid (50168 bp, NZ_CP048321.1)	
CF064[56]	surface water	Switzerland	2019	ST940	*qnrS1* (type M)	IncX3/ColKP3 plasmid (50136 bp, NZ_CP048325.1)	SDSE (0)
CF142[56]	surface water	Switzerland	2019	ST648	*qnrS1* (type M), *qnrB4, aac(6')-Ib-cr*	*qnrS1*, *qnrB4*: IncF/ColKP3 plasmid (155486 bp, NZ_CP048338.1) *aac(6')-Ib-cr*: chromosome (5073188 bp, NZ_CP048337.1)	LNIE (3)
CF061[56]	surface water	Switzerland	2019	ST940	*qnrS1* (type M)	IncX3/ColKP3 plasmid (51471 bp, NZ_CP048327.1)	SDSE (0)
CF010[56]	surface water	Switzerland	2019	ST656	*qnrS1* (type M)	IncX3/ColKP3 plasmid (51479 bp, NZ_CP048332.1)	LDSE (1)
CF124[56]	surface water	Switzerland	2019	ST410	*qnrS1* (type M)	IncX3/ColKP3 plasmid (51466 bp, NZ_CP048346.1)	LNIE (3)
CF053[56]	surface water	Switzerland	2019	ST205	*qnrB4*	IncF plasmid (144585 bp, NZ_CP048360.1)	LNIE (3)
CF164[56]	surface water	Switzerland	2019	ST167	*aac(6')-Ib-cr*	IncF plasmid (132482 bp, NZ_CP048368.1)	LNIE (3)

CF038[56]	surface water	Switzerland	2019	ST410	*aac(6')-Ib-cr*	IncF plasmid (86996 bp, NZ_CP048377.1)	LNIE (3)
TKEC21-17[57]	municipal wastewater	Turkey	2021	ST609	*qnrS1* (type A), *qnrS1* (type L)	*qnrS1* (type A): IncF plasmid (91489 bp, NZ_CP092450.1) *qnrS1* (type L): IncX3 plasmid (46799 bp, NZ_CP092451.1)	SDSE (0)
TKEC21-59[57]	municipal wastewater	Turkey	2021	ST609	*qnrS1* (type A)	IncF plasmid (86914 bp, NZ_CP092453.1)	SDSE (0)
1000C-3[58]	hospital wastewater	USA	2018	ST167	*aac(6')-Ib-cr*	IncF plasmid (145445 bp, NZ_CP091428.1)	LNIE (3)

[a]Detailed information on each isolate, such as other AMR genes detected, is available in **Table S2**.

[b]The context type is shown for *qnrS1*.

[c]GyrA codons 83 and 87 and ParC codons 80 and 84 are shown in this order. The number of amino acid substitutions is shown in parentheses.

592 **FIGURES**

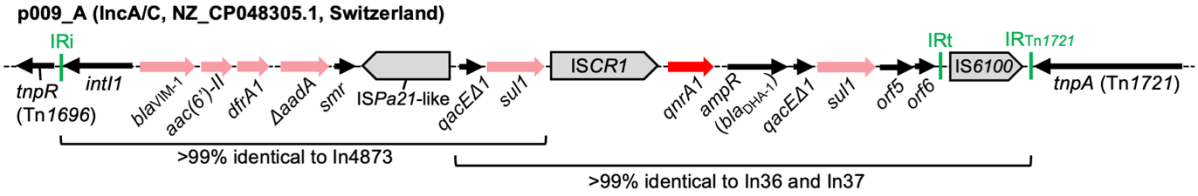

593

594 **Figure 1**. The genetic context of *qnrA1*. A red arrow indicates the TMQR determinant, pink

595 arrows indicate other AMR genes, gray pointed boxes indicate ISs, and black arrows indicate

596 other genes. Diagrams are not exactly to scale (this also applies to other figures). Inc type,

597 nucleotide accession number, and country of origin are shown in parentheses next to the

598 plasmid name. IR: inverted repeat. IRi: inverted repeat at *intI1* end. IRt: inverted repeat at *tni*

599 end.

600

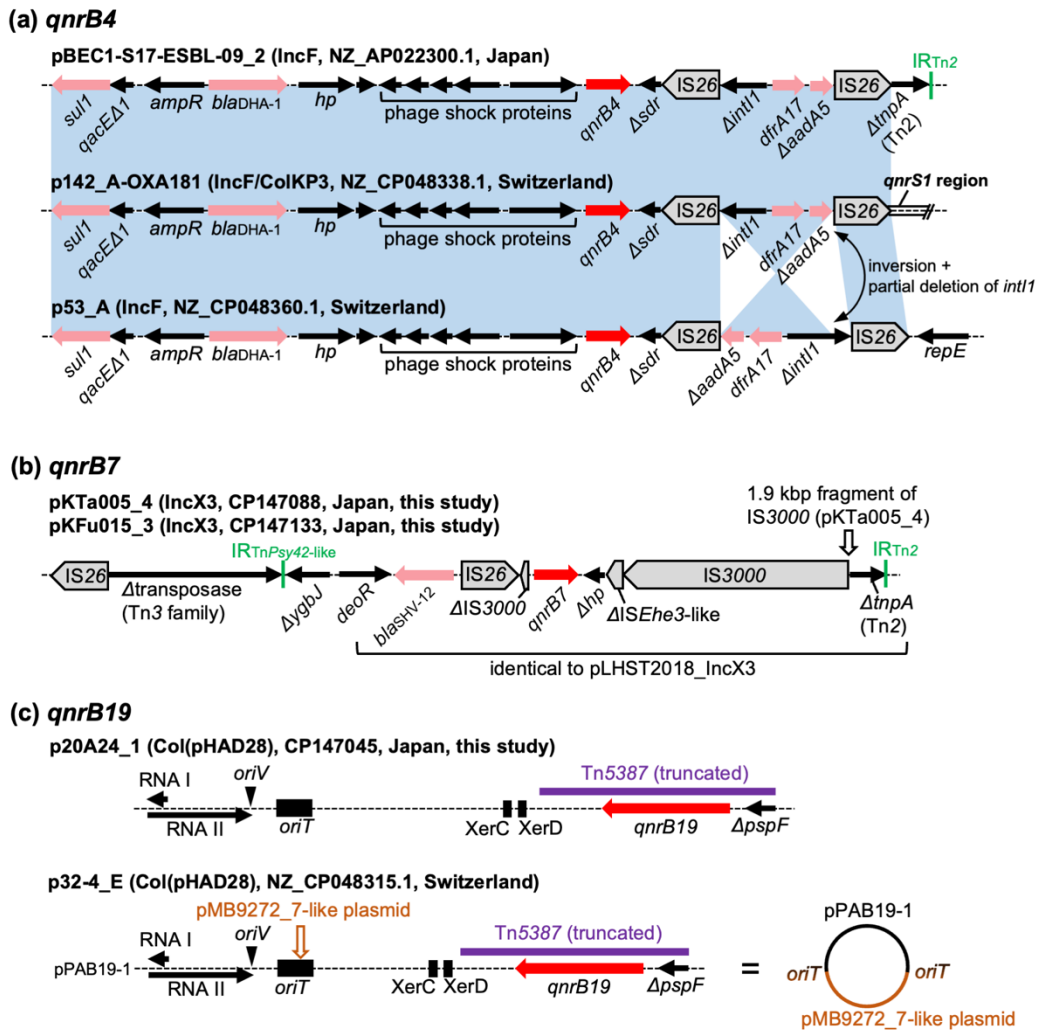

Figure 2. Genetic contexts of (a) *qnrB4*, (b) *qnrB7*, and (c) *qnrB19*. Genes and elements are shown as in **Figure 1**. Nucleotide sequences with >99% nucleotide identity are indicated by the blue shaded regions in panel (a). Panel (c) is enlarged compared with panels (a) and (b), and describes the whole plasmid structures. For p32-4_E, a circular structure is also shown to describe the relationship to pPAB19-1 and the pMB9272_7-like plasmid. The putative *oriT* sequence in the pMB9272_7-like plasmid was predicted by comparison with well-characterized plasmids such as ColE1. hp: hypothetical protein.

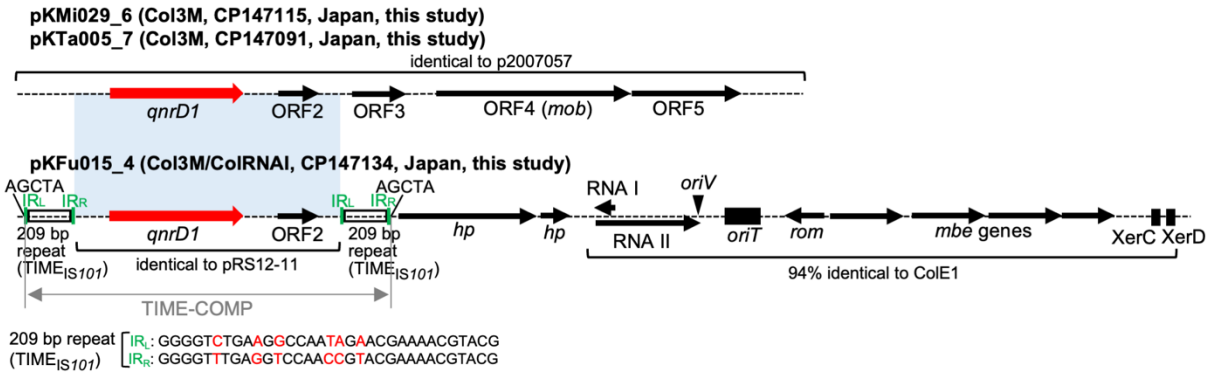

610

611 **Figure 3**. Structures of plasmids carrying *qnrD1*. Genes and elements are shown as in earlier

612 figures. The light blue shaded regions indicate nucleotide sequences with ~95% nucleotide

613 identity. Annotation of pKFu015_4 was partially performed by sequence comparison with

614 ColE1. IR_L: inverted repeat left. IR_R: inverted repeat right. IR_L and IR_R of $TIME_{IS101}$ are shown

615 at the bottom of the figure, and different nucleotides are marked in red.

616

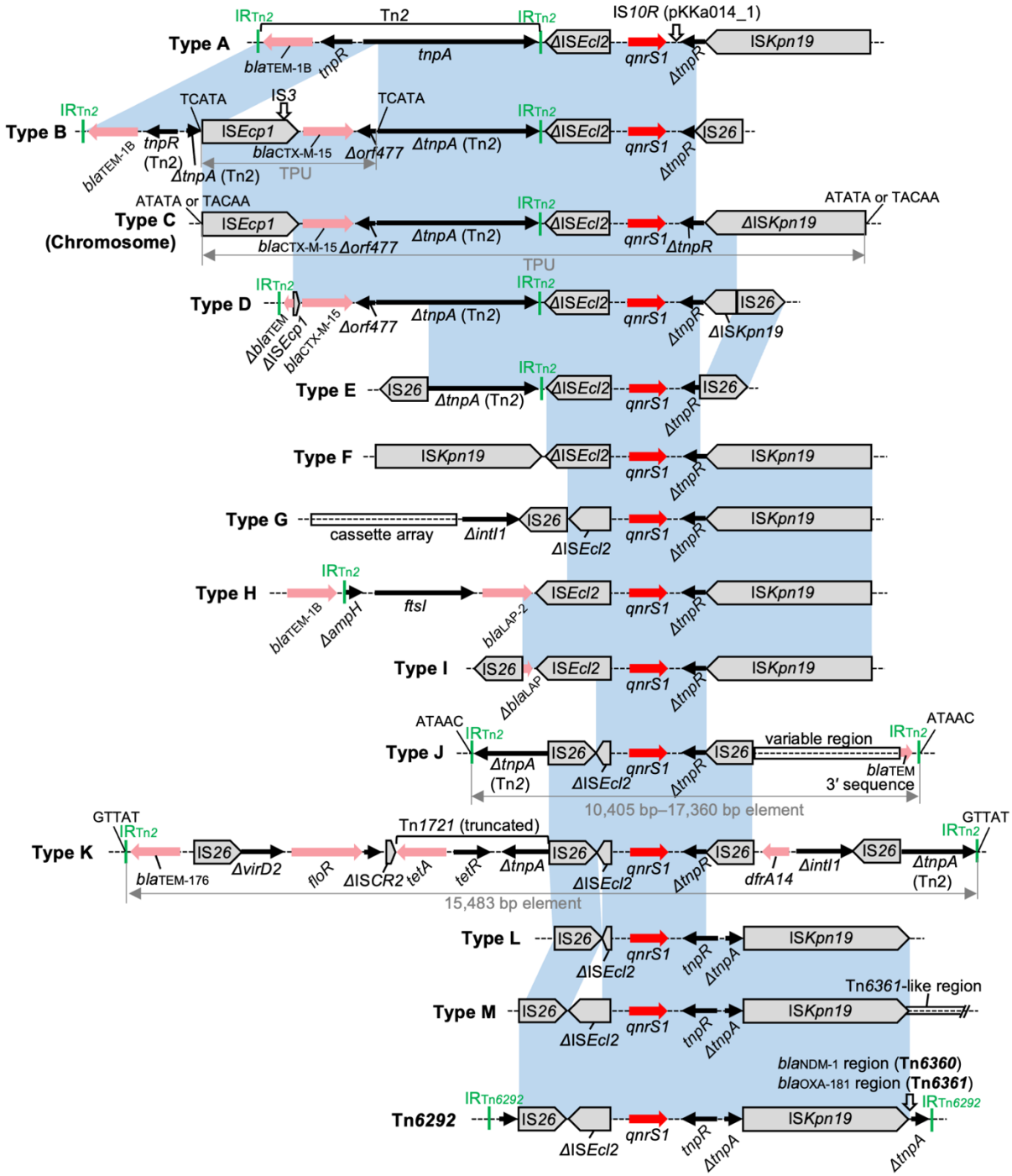

617

618 **Figure 4**. Genetic contexts of *qnrS1*. Genes and elements are shown as in earlier figures. The

619 blue shaded regions indicate nucleotide sequences with >99% nucleotide identity. Note that for

620 simplicity, only *qnrS1* and directly flanking regions without complex rearrangements (such as

621 inversions) are shaded in blue (e.g., the left IS*Kpn19* in the type F context shares >99%

622 nucleotide identity with IS*Kpn19* in the type G context, but this region is not shaded). Tn*6292*

623 and its derivatives (Tn*6360* and Tn*6361*) are shown for the purpose of comparison. See **Table**

624 **1** for information on genomes carrying each context type.

625

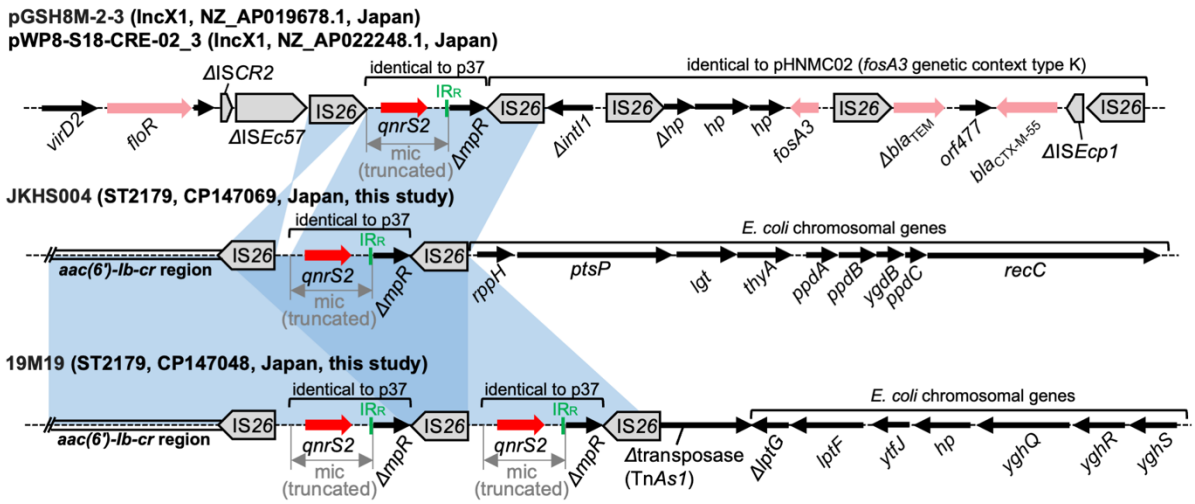

626

627 **Figure 5**. Genetic contexts of *qnrS2*. Genes and elements are shown as in earlier figures.

628 JKHS004 and 19M19 carry *qnrS2* on the chromosome, and chromosomal STs are indicated

629 instead of plasmid types. The blue shaded regions indicate nucleotide sequences with >99%

630 nucleotide identity.

631

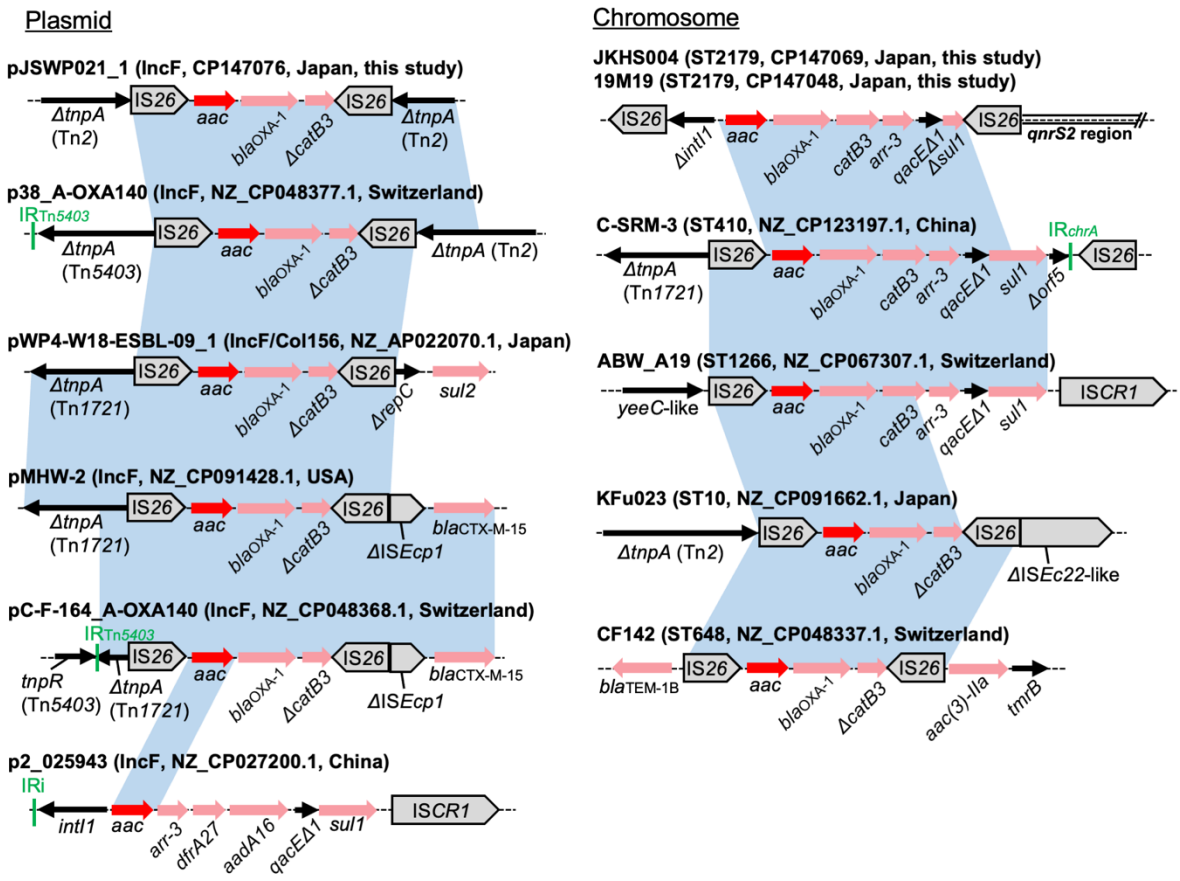

632

633 **Figure 6**. Genetic contexts of *aac(6')-Ib-cr*. The contexts are shown separately for plasmids

634 and chromosomes. *aac(6')-Ib-cr* is abbreviated as *aac* in the figure. Genes and elements are

635 shown as in earlier figures. The blue shaded regions indicate nucleotide sequences with >99%

636 nucleotide identity. Note that for simplicity, only *aac(6')-Ib-cr* and flanking regions are shaded

637 in blue (e.g., IS*26* sequences in JKHS004 and 19M19 share >99% nucleotide identity to IS*26*

638 sequences in C-SRM-3, but these regions are not shaded).

639

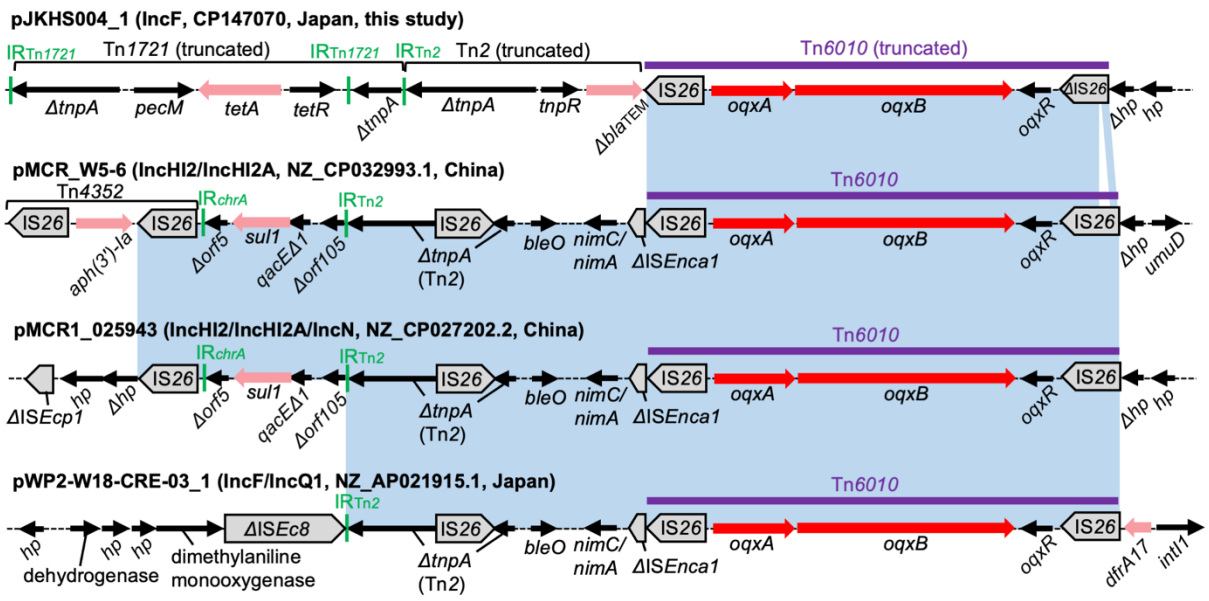

640

641 **Figure 7**. Genetic contexts of *oqxAB*. Genes and elements are shown as in earlier figures. The

642 blue shaded regions indicate nucleotide sequences with >99% nucleotide identity. Note that for

643 simplicity, only Tn*6010* and flanking regions are shaded in blue (e.g., the left IS*26* in Tn*4352*

644 shares >99% nucleotide identity to other IS*26* sequences, but these regions are not shaded).

645

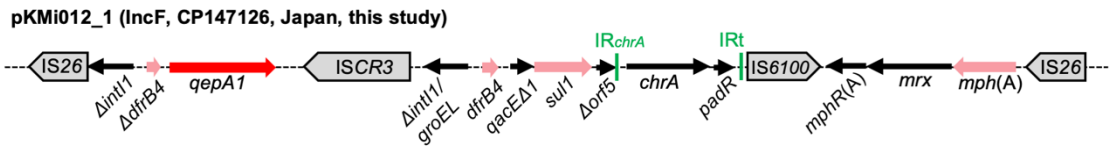

646

647 **Figure 8**. The genetic context of *qepA1*. Genes and elements are shown as in earlier figures.

648